Mutagenesis, 2018, 33, 77–85
doi:10.1093/mutage/gex027
Original Manuscript
Advance Access publication 7 October 2017

OXFORD

Original Manuscript

Size-dependent genotoxicity of silver, gold and platinum nanoparticles studied using the mini-gel comet assay and micronucleus scoring with flow cytometry

Jana Lebedová[1,2], Yolanda S. Hedberg[3], Inger Odnevall Wallinder[3] and Hanna L. Karlsson[1,*]

[1]Institute of Environmental Medicine, Karolinska Institutet, Nobels väg 13, 171 77 Stockholm, Sweden, [2]RECETOX, Masaryk University, Kamenice 753/5, pavilon A29, CZ62500 Brno, Czech Republic, [3]School of Chemical Science and Engineering, Department of Chemistry, Division of Surface and Corrosion Science, KTH Royal Institute of Technology, Drottning Kristinas väg 51, 100 44 Stockholm, Sweden

*To whom correspondence should be addressed. Tel: +46 8 524 87576; Fax: + 46 8 33 69 81; Email: Hanna.L.Karlsson@ki.se

Received 13 June 2017; Editorial decision 29 August 2017; Accepted 22 September 2017.

Abstract

Metallic nanoparticles (NPs) are promising nanomaterials used in different technological solutions as well as in consumer products. Silver (Ag), gold (Au) and platinum (Pt) represent three metallic NPs with current or suggested use in different applications. Pt is also used as vehicle exhaust catalyst leading to a possible exposure via inhalation. Despite their use, there is limited data on their genotoxic potential and possible size-dependent effects, particularly for Pt NPs. The aim of this study was to explore size-dependent genotoxicity of these NPs (5 and 50 nm) following exposure of human bronchial epithelial cells. We characterised the NPs and assessed the viability (Alamar blue assay), formation of DNA strand breaks (mini-gel comet assay) and induction of micronucleus (MN) analysed using flow cytometry (*in vitro* microflow kit). The results confirmed the primary size (5 and 50 nm) but showed agglomeration of all NPs in the serum free medium used. Slight reduced cell viability (tested up to 50 μg/ml) was observed following exposure to the Ag NPs of both particle sizes as well as to the smallest (5 nm) Au NPs. Similarly, at non-cytotoxic concentrations, both 5 and 50 nm-sized Ag NPs, as well as 5 nm-sized Au NPs, increased DNA strand breaks whereas for Pt NPs only the 50 nm size caused a slight increase in DNA damage. No clear induction of MN was observed in any of the doses tested (up to 20 μg/ml). Taken together, by using the comet assay our study shows DNA strand breaks induced by Ag NPs, without any obvious differences in size, whereas effects from Au and Pt NPs were size-dependent in the sense that the 5 nm-sized Au NPs and 50 nm-sized Pt NPs particles were active. No clear induction of MN was observed for the NPs.

Introduction

Metallic nanoparticles (NPs) are promising nanomaterials used in many different technical solutions including consumer products and biomedical applications. Among the engineered nanomaterials, silver NPs (Ag NPs) are most commonly incorporated in nano-functionalised consumer products, mainly due to their antimicrobial properties. The global consumption of Ag NPs has been estimated to be hundreds of tons per year and the different products include paints, cosmetics, deodorants, clothing, textiles, food packaging, medical devices, wound dressings, detergents, biosensors and biomedical products (1). Gold (Au) NPs are also increasingly used in various biomedical applications including imaging, therapeutics and molecular sensing (2). A third metal with possible human

exposure in its NP-form is platinum (Pt) that, e.g. is used as vehicle exhaust catalyst (3). All three metallic NPs (Ag, Au and Pt) have been suggested to be of therapeutic use in different applications (4). Altogether, their increased use in different applications suggests an increased risk for human exposure.

Of these three metallic nanomaterials, Ag NPs are the most widely studied in terms of genotoxicity. Both *in vitro* (5–10) and *in vivo* (11,12) studies have shown genotoxicity. How the particle size contributes to the genotoxic effects is, however, still unclear. Some studies indicate rather similar extent of DNA breaks for various sizes of Ag NPs (8,13), whereas a higher genotoxic potency of smaller Ag NPs (when using mass as a dose metric) is supported by several studies (9,14–16). Genotoxicity of Au NPs is still a controversial question and Au NPs are generally regarded as bio-inert (2). Still, some studies have shown genotoxic effects (17,18). The number of studies examining Pt NPs is very limited, but two studies have reported some genotoxicity (5,19). However, Elder and colleagues reported that Pt NPs do not induce oxidative stress or cytotoxicity in either cell-free systems, cultured human cells or when tested *in vivo* (20).

Due to the inconsistencies in previous studies for all these NPs and limited available scientific data for Pt NPs, we focused the present study on revealing possible size-dependent genotoxic effects of Ag, Au and Pt NPs. Human bronchial epithelial cells (HBEC) were used since we were particularly interested in lung genotoxic effects following inhalation of Pt NPs.

Materials and methods

NPs and characterisation of size

All NPs (Ag, Au and Pt) investigated in this study were citrate coated (BioPure™) and in two particle sizes, 5 and 50 nm. The NPs were obtained from nanoComposix (San Diego, CA) in the form of stock dispersions (1 mg/ml) in aqueous 2 mM citrate (Ag and Pt) and in ultrapure water (milli-Q) (Au). The size of the NPs was examined in a Hitachi HT 7700 (Hitachi, Tokyo, Japan) electron microscope at 80 kV and digital images was taken by a Veleta camera (Olympus, Münster, Germany). The size of particles was measured using the software in the microscope (Olympus Soft Imaging Solutions, GmbH, Münster, Germany). A Nanosight NS300 instrument (Malvern, Uppsala, Sweden) with a 405 nm laser was used for NP tracking analysis (NTA) in order to determine the hydrodynamic number distribution of all NPs in the exposure medium (mix of LHC-9 and PRMI, see below) at particle concentrations of 10 µg/ml. All NPs were scattering the light at very high intensities, why the camera level of the instrument had to be adjusted to very low levels (4–6 as compared with 11–13 for the background). Each measurement was performed at 25°C and with 3 times 60 s captures. The NTA 3.2 software was employed and the viscosity of water was used as input value.

Characterisation and calculation of electrophoretic mobility and zeta potential

The electrophoretic mobility of the NPs was measured by means of a Zetsasizer nano Z instrument (Malvern, Uppsala, Sweden) at a ratio of 5 µg NPs in 1 ml 14 mM NaCl (pH 5.4) in Malvern Zetasizer Nanoseries cuvettes. Prior to the measurement, the solution was mixed using a vortex shaker. The Smoluchowski approximation was used to calculate the zeta potential from the electrophoretic mobility, with the input values of 0.20, 0.135 and 4.5 as the refractive index for Au, Ag and Pt NPs, respectively. As a dispersant, water with a refractive index of 1.33, a viscosity of 0.8872 cP and a dispersant dielectric constant of 78.5, was used for calculations. Since the Smoluchowski approximation not always is the best model to describe metal NPs in solution (21), the electrophoretic mobility is presented in the Supplementary Material.

Cell culture conditions and exposures

The normal human bronchial epithelial cells HBEC3-kt, immortalised with CDK4 and hTERT were used for all experiments in this study. This cell line, hereafter denoted HBEC, was a kind gift from S. Zienolddiny, STAMI (Statens Arbeidsmiljøinstitutt) Norway via collaborations in the FP-7 NANoREG consortia. HBEC cells were cultured in 50% of LHC-9 serum free medium (Gibco 12680013, supplemented with 1% penicillin-streptomycin, PEST) and 50% of RPMI 1640 medium (Sigma R8758 supplemented with 1% PEST and 1% l-glutamine). No fetal bovine serum (FBS) was added into the cell medium. Cells were cultured in flasks pre-coated with 0.01% collagen (Type I, PureCol® from Advanced BioMatrix) in a humidified atmosphere at 37°C, 5% CO_2 and sub-cultured at 80% confluence. For each assay, cells were seeded 1 day prior the experiment at an approximate density of 1.5–2 ×·10^4 cells/cm^2. The exposure took place the following day at approximately 60–80% cell confluency. The stock suspensions of NPs were vortexed, the correct amount added to cell medium in Eppendorf tubes and the suspensions were vortexed again before addition to the cells.

Cell viability assessment

Cell viability was assessed by the Alamar Blue assay, a method based on analysis of the reducing power of metabolically active cells. HBEC cells were seeded in transparent 96 well plates pre-coated with 0.01% collagen 1 day prior to exposure. The cells were then exposed to Ag, Au and Pt NPs in two sizes (5 and 50 nm) in concentrations ranging from 0.5 to 50 µg/ml in 100 µl medium (0.14–14 µg/cm^2) for 48 h. After exposure, 10% Alamar Blue reagent (Invitrogen) was added to each well and incubation was performed for 2 h at 37°C. The fluorescence (Ex560/Em590) was measured by using a plate reader (Tecan Infinite T200) equipped with Magellan software. After reading, Alamar Blue reagent was removed and fresh culture media without NPs was added to each well for additional 24 h. Fresh Alamar Blue reagent was then added and fluorescence was again measured as described above. Results are presented as percentage of cell viability compared to control, which was set to 100%. Background fluorescence (10% Alamar Blue in medium) was subtracted from each well. Experiments were performed four times in duplicate wells for each particle type, size, time point and concentration.

Genotoxicity assessment using mini-gel comet assay

The alkaline comet assay, also known as single cell gel electrophoresis, was used to detect single and double DNA strand breaks as well as alkali labile sites. HBEC cells were seeded in 24-well plates and exposed to Ag, Au and Pt NPs (5 and 50 nm) in concentrations 1, 10 and 20 µg/ml in 600 µl medium (0.3–6.3 µg/cm^2) for 48 h. Cells were harvested and the mini-gel comet assay was performed similarly to the method previously described (22). Briefly, cells were harvested using trypsin, cell medium (150 µl) with FBS was added to stop trypsinisation and 25 µl of the cell suspension was mixed with 150 µl 0.75% low melting point agarose (type VII from Sigma-Aldrich). Next, 20 µl aliquots were added as drops onto cold microscope slides pre-coated with 0.3% agarose. Two

gels on different slides were made for each sample and eight mini-gels were prepared on each slide. Cells were lysed on ice with a freshly prepared 1% Triton X-100 lysis buffer (2.5 M NaCl, 0.1 M EDTA, 10 mM Tris, pH 10) for 1 h in dark conditions. They were then placed in alkaline buffer (0.3 M NaOH, 1 mM EDTA) for unwinding (40 min). Afterwards, electrophoresis was performed in the same buffer for 30 min at 29 V, 1.15 V/cm. Samples were then neutralised (2 × 5 min in 0.4 M Tris buffer and 5 min in water), dried overnight and fixed in methanol (5 min). DNA was stained by immersing air-dried slides in 1:10 000 SYBR-green (Thermo Fisher Scientific, Waltham, MA) diluted in 1× TAE buffer (Sigma–Aldrich) for 15 min. Scoring was then performed using a fluorescence microscope (Leica DMLB, Meyer Instruments, Inc., Houston, TX) with the Comet assay IV software (Perceptive Instruments Ltd., Suffolk, UK). One hundred cells were scored per sample (50 comets on each duplicate gel) and results were expressed as mean of percent DNA in tail. Exposure to hydrogen peroxide (20 µM) for 5 min was used as a positive control. Three individual experiments were performed for each particle and concentration.

Genotoxicity assessment using micronucleus assay

The induction of micronuclei was determined by flow cytometry using the *in vitro* microflow kit (Litron Laboratories). The method is based on double staining in order to distinguish between apoptotic/necrotic cells and damaged cells with micronuclei. The method was performed according to instructions given by the manufacturer and as described previously (22). HBEC cells were

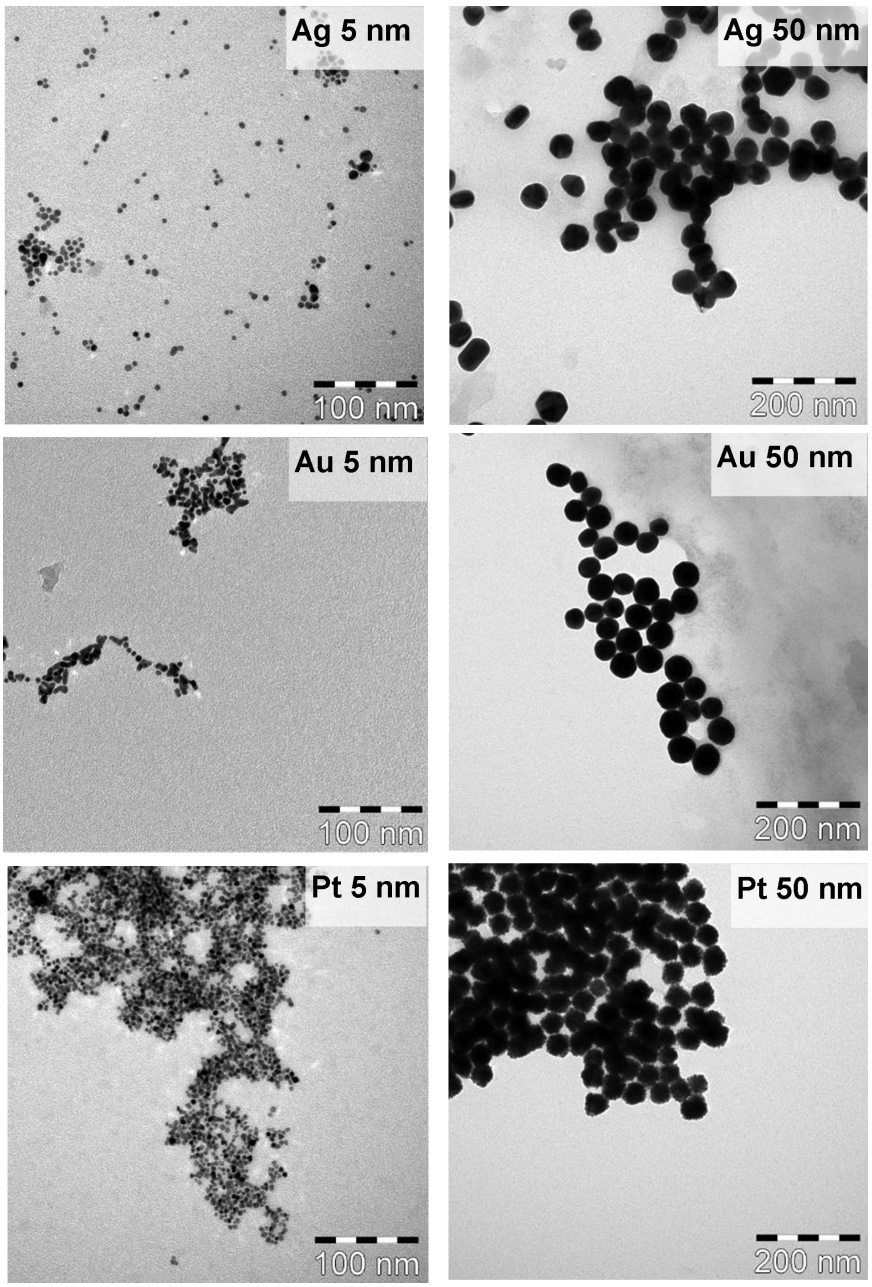

Figure 1. TEM images of the NPs included in the study. The NPs shown are Ag NPs (upper), Au NPs (middle) and Pt NPs (lower). The bars for the 5 nm NPs (left) indicate 100 nm and for the 50 nm NPs (right) 200 nm.

seeded in 96-well plates and exposed to 1, 10 and 20 µg/ml of NPs (Ag, Au and Pt; 5 and 50 nm) in 100 µl (0.3–6.3 µg/cm^2) for 48 h. After exposures, the cells were washed twice with phosphate-buffered saline (PBS) and incubated on ice with ethidium monoazide stain (EMA) for 30 min under cold white light to allow stain photoactivation. Subsequently, cells were lysed and stained with SYTOX green for 1.5 h in dark conditions and 37°C. Samples were then acquired using a BD Accuri C6 flow cytometer (Becton Dickinson). The flow was set to 20 µl/min and run threshold to 10 000 gated nuclei. Gating of the healthy nuclei, micronuclei, apoptotic/necrotic nuclei together with analysis of the plots and cell cycle histograms was performed using the BD Accuri C6 software. Etoposide (0.2 µg/ml) was used as a positive control.

Statistics

Statistical analysis was performed using GraphPad Prism 5 statistical software (GraphPad Inc.). Two-way analysis of variance (ANOVA) was used to test whether the effects analysed were statistically significantly depending on concentration and/or size. The Alamar blue assay was performed in four independent experiments with two different wells exposed in each experiment ($N = 8$). The comet assay was performed in three independent experiments with one well exposed per sample ($N = 3$). Two different separate gels were prepared from each sample. The micronucleus (MN) assay was performed in three independent experiments with two different wells exposed in each experiment ($N = 6$). All results are expressed as mean values ± SEM.

Results

Particle characterisation

The NPs were characterised in terms of size (using TEM), zeta potential (calculated from electrophoretic mobility, see Supplementary Table 1) as well as size of the NPs in the actual cell medium (using NTA). The results confirmed the size as reported by the manufacturer, approximately 5 and 50 nm, respectively, (see Figure 1) and results in Table 1 show the mean and standard deviation of at least 100 measured NPs. Zeta potential measurements showed that all NPs had a negative surface charge in the stock suspension. These results are presented in Table 1 as average and standard deviation values of at least two independent samples with three replicate readings (see also electrophoretic mobility in the Supplementary Material). Information about surface area and endotoxin content provided by the manufacturer (nanoComposix) is also given in Table 1. The NTA analysis showed that all NPs agglomerated in the cell medium as they all showed size distributions up to approximately 400 nm (Figure 2). For all NPs, the 50 nm sized particles seemed to have some fraction of primary sized (50–80 nm) NPs in suspension, however, with the majority of NPs present as larger (agglomerated) sizes. In contrast, all 5 nm NPs showed size distributions that were significantly larger as compared to their primary size (>70 nm for Ag NPs, >100 nm for Au NPs and >80 nm for Pt NPs). It should, however, be noted that the primary NPs, sized <10 nm may be difficult to detect, as they are overshadowed by the larger agglomerates. The most evident peak that could be assigned to the primary particle size was observed for the 50 nm-sized Ag NPs.

Cell viability

The NPs were in general non-cytotoxic in the doses tested (up to 50 µg/ml) at 48 h. Both the 5 and 50 nm-sized Ag NPs showed only a slight reduction in cell viability at the highest dose tested (87% and 90% viability for the 5 and 50 nm, respectively, see Supplementary Figure 1). The effect of cell viability was more pronounced when the reading was performed after additional 24 h in fresh medium (73% and 63% viability, respectively). Two-way ANOVA analysis showed evident concentration dependent effects ($P < 0.001$), but no size-dependent effects (Figure 3A). This was in contrast to the Au NPs that showed a slight (statistical significant) reduction in cell viability for the smallest Au NPs (5 nm, 78% viability in 50 µg/ml) whereas the 50 nm-sized particles resulted in higher cell viability compared to controls (107% viability in 50 µg/ml) at 48 h + 24 h (Figure 3B). A similar trend was observed for the Pt NPs showing 97% viability in the highest dose for the 5-nm sized particles and 109% viability (most likely due to increased proliferation) for the 50 nm-sized Pt NPs (Figure 3C).

DNA strand breaks—comet assay

The mini-gel alkaline comet assay was used to detect DNA strand breaks in the HBEC cells following 48 h exposure to the six different NPs in three doses (1, 10 and 20 µg/ml; 0.3–6.3 µg/cm^2) (Figure 4). Compared to the control levels (2.6% DNA in tail), the Ag NPs showed increased DNA breaks in all doses with levels around 8–9% DNA in tail for particles sized 5 nm and around 4–11% for particles sized 50 nm. Analysis using two-way ANOVA for the Ag NPs showed concentration-dependent effects but no size-dependent effects (both particle sizes being active). This was in contrast to the Au NPs for

Table 1. Summary of particle characteristics of the investigated NPs of Ag, Au and Pt sized 5 and 50 nm

		Size (TEM, nm)	Surface area[a] (TEM, m^2/g)	Endotoxin[a] (EU/ml)	Zeta potential[b] (mV)	Size in cell medium[g] (NTA, nm)
Ag	5 nm	5.2 ± 1.1	103.2	<5	-35 ± 6.9[c]	70–300 (multiple peaks)
	50 nm	47.3 ± 5.8	11.0	<2.5	-37 ± 9.6[d]	50 (120–350)
Au	5 nm	5.2 ± 0.9	60.6	<5	-30 ± 4.2[e]	100, 220 and 300
	50 nm	49.2 ± 6.2	5.9	<2.5	-37 ± 7.8	80, 120, 200, 300
Pt	5 nm	4.8 ± 0.8	56.4	<2.5	-43 ± 2.1	80–450 (multiple peaks)
	50 nm	44.3 ± 4.6	5.9	<2.5	-29 ± 2.5[f]	70–380 (multiple peaks)

[a]Information on surface area and endotoxin content provided by the manufacturer (nanoComposix).
[b]Zeta potential calculated from electrophoretic mobility (see supplement) of NPs (5 µg NPs/ml) in 14 mM NaCl (pH 5.4).
[c]Three main peaks at -37, -16 and -26 mV.
[d]Two main peaks at -21 and -47 mV.
[e]Broad zeta potential distribution from -70 to +40 mV with two main peaks at -30 and -11 mV.
[f]Broad zeta potential distribution from -95 to +20 mV with one main peak at -29 mV.
[g]Particle size in cell medium was determined using NTA, the main peaks (nm) are indicated.

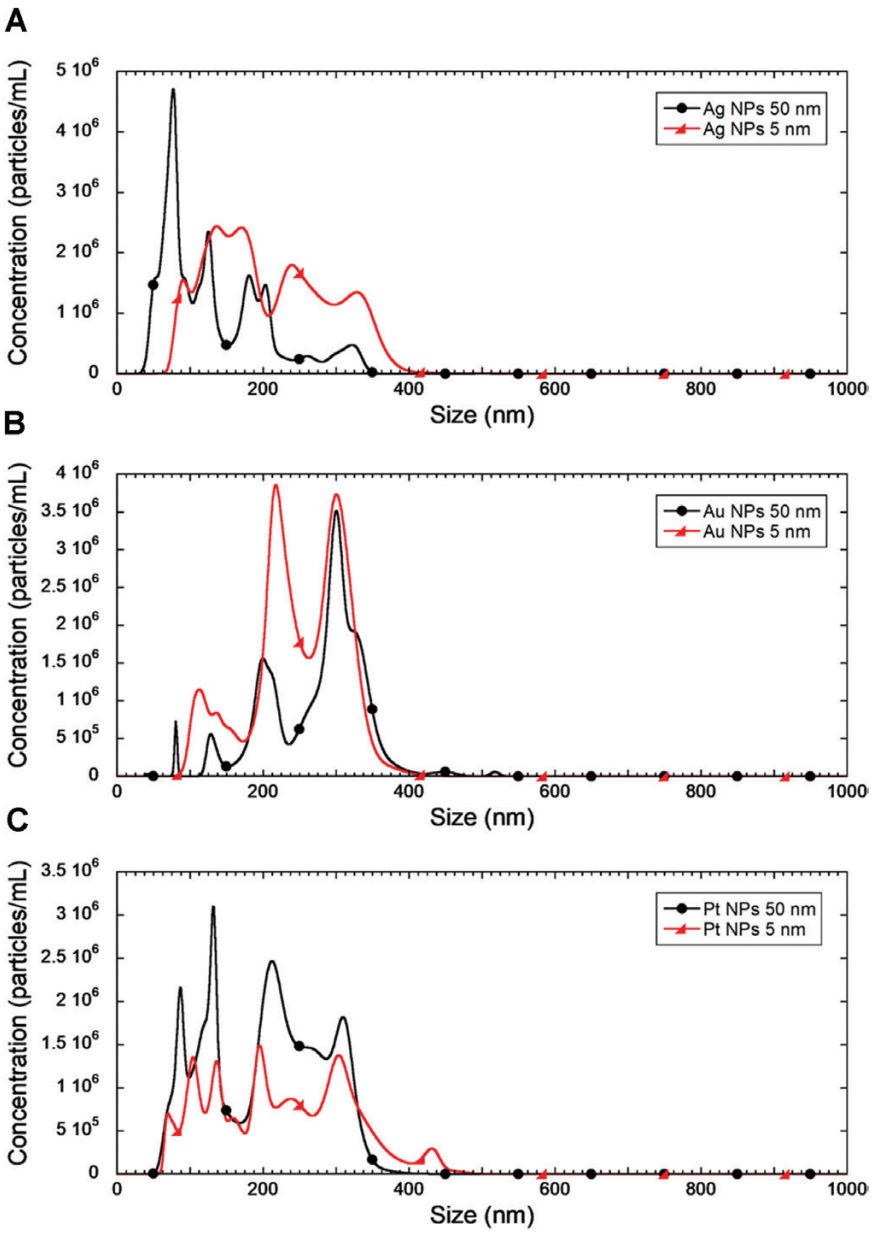

Figure 2. Size of the six different NPs in serum free cell medium (50% LHC-9 and 50% RPMI-1640), determined by means of nano tracking analysis (NTA). All NPs; Ag (A), Au (B) and Pt (C) agglomerated to a large extent. Particle sizes ≤5 nm might be undetectable due to a low camera level required as a result of large, intensively scattering agglomerates.

which only the smallest particles (5 nm) were active showing 3.3, 5.6 and 7.2% DNA in tail, respectively, in the different concentrations tested. The Pt NPs showed a slight size-dependent effect in the sense that Pt 50 nm caused some DNA damage not observed for the 5 nm-sized ones, but there was no significant concentration-dependent effect. When comparing the NPs of the same size pairwise using two-way ANOVA, Ag NPs were significantly more active compared to Au and Pt both for 5 and 50 nm. The positive control (cells treated with 20 µM H_2O_2 for 5 min on ice) showed increased DNA strand breaks in all experiments.

MN induction

MN induction was analysed by using flow cytometry following exposure to 1, 10 and 20 µg/ml (0.3–6.3 µg/cm^2) of the six different NPs for 48 h (Figure 5). The control cells showed 1.7% MN and, except from a minor increased induction observed for the Ag NPs sized 5 nm (2.1% in the middle and high dose), no effects were observed. The positive control etoposide (0.2 µg/ml) resulted in an induction of approximately 15% MN.

Discussion

In this study, we explored size-dependent genotoxicity of three metallic NPs; Ag, Au and Pt with primary sizes of 5 and 50 nm, following exposure of human bronchial epithelial cells. The main reason for choosing airway cells was the lack of data for Pt NPs, and since increased levels of Pt have been observed in airborne dust (23), inhalation may be an important exposure route for the

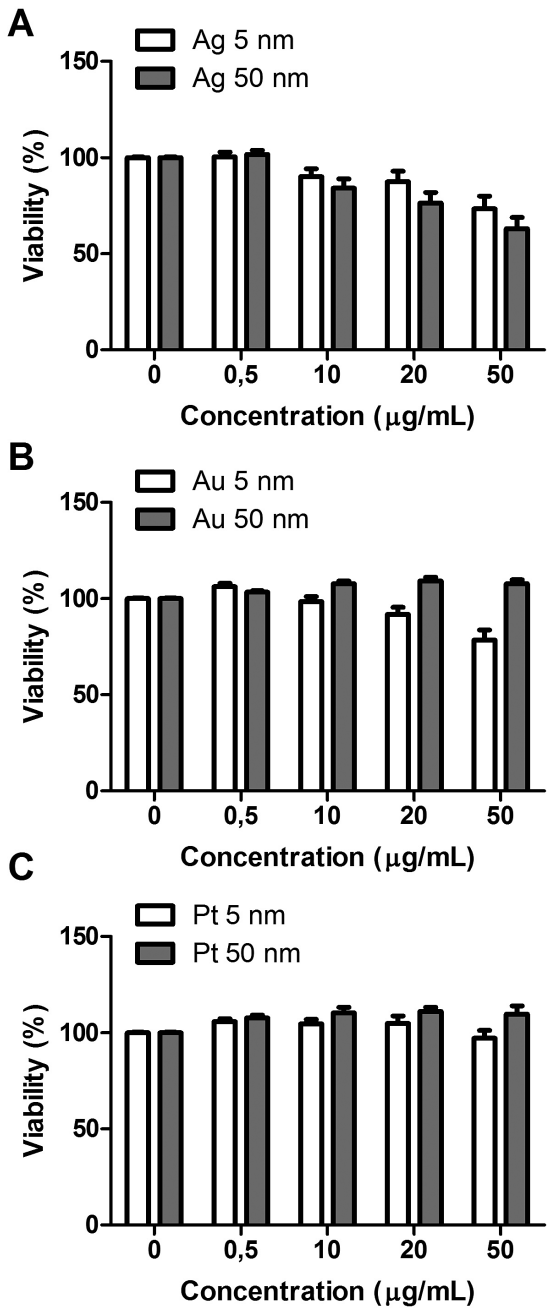

Figure 3. Viability of the HBEC cells following exposure to Ag, Au and Pt NPs. The cells were exposed to the different NPs in primary size 5 and 50 nm, respectively, for 48 h and were then cultured for another 24 h in fresh medium. After this, the viability was analysed using the Alamar Blue assay. Analysis using two-way ANOVA showed concentration dependent effects for Ag NPs ($P < 0.001$) and size-dependent effects for Au NPs.

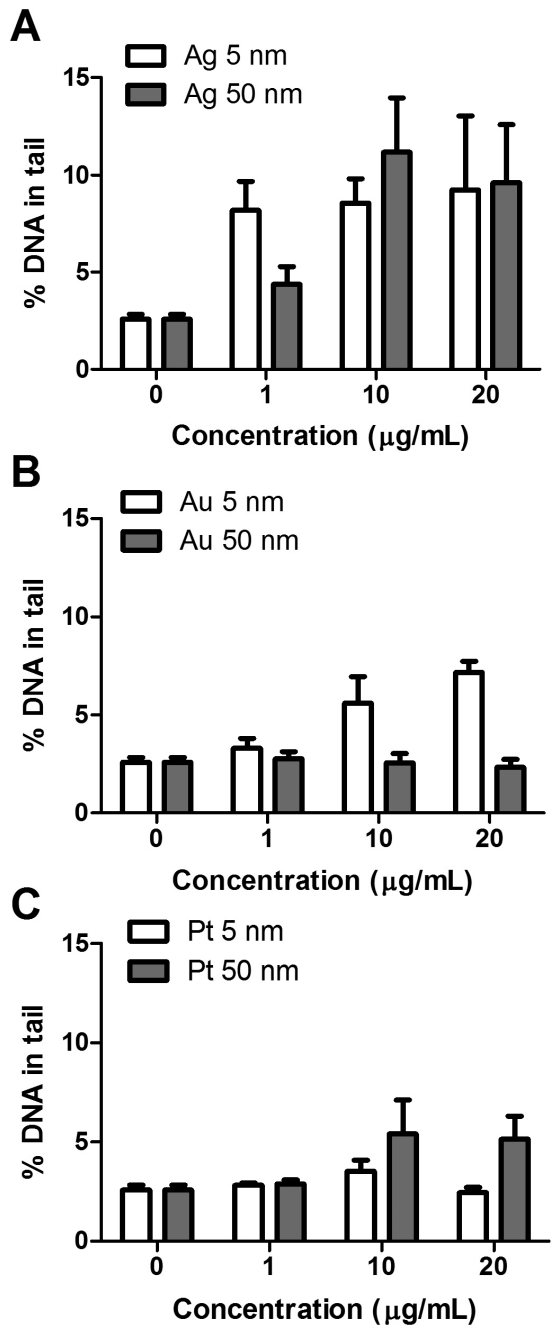

Figure 4. DNA damage (comet assay) following exposure to Ag, Au and Pt NPs. The HBEC cells were exposed to 1, 10 and 20 μg/ml (0.3–6.3 μg/cm^2) of the different NPs in primary sizes 5 and 50 nm, respectively, for 48 h after which the comet assay was performed. Analysis using two-way ANOVA showed concentration-dependent effects for Ag NPs, and concentration as well as size-dependent effects for Au NPs. The Pt NPs showed no statistical significant effects. The positive control (cells treated with 20 μM H_2O_2 for 5 min) showed increased DNA strand breaks in all experiments.

general population. We employed two of the most commonly used methods for assessing genotoxicity—the comet assay and the MN assay. By using the mini-gel comet assay (with eight gels on each comet slide) as well as a 96-well microplate-based flow cytometric analysis of micronuclei, time-saving versions of these methods were employed. This enabled screening of all six different NPs in different doses in the same study. Indeed, MN detection using flow cytometry has emerged as an efficient way of determining MN formation (24). One potential problem with the method is how to distinguish between MN and apoptotic bodies. With the current version, however, a dual dye sequential staining procedure enables their discernment. Thus, cells are first incubated with EMA, a nucleic acid that enters the compromised membranes of necrotic and late-stage apoptotic cells, and then with a detergent-containing lysis solution that includes the nucleic acid dye SYTOX green. In this way, EMA-positive cells (representing dying cells) can be

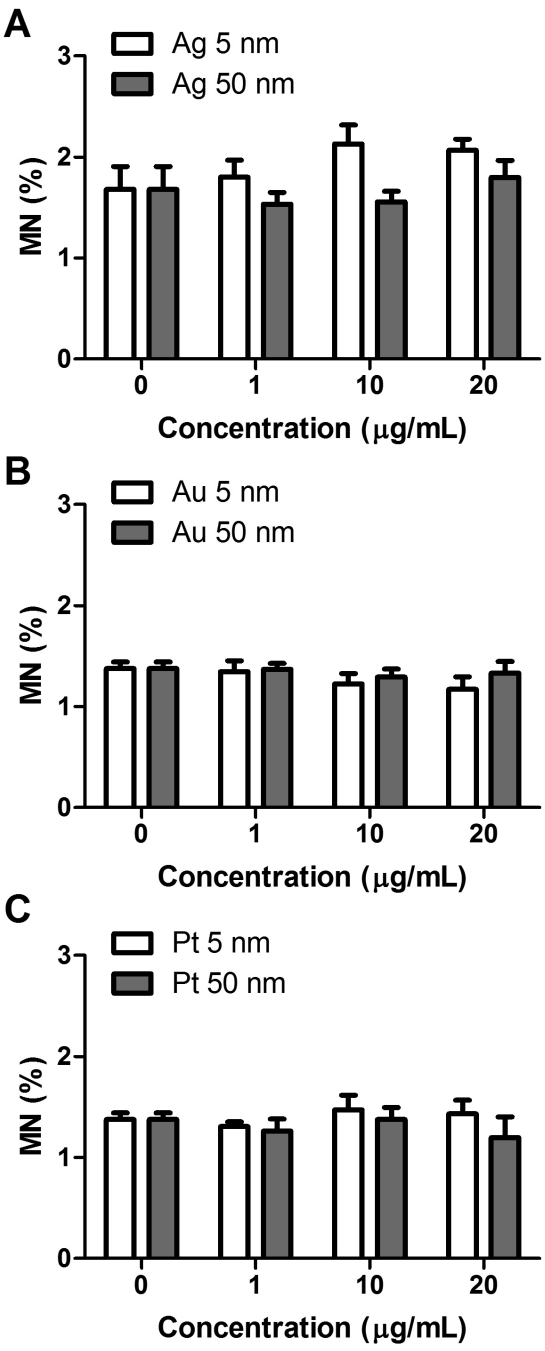

Figure 5. Micronucleus induction following exposure to Ag, Au and Pt NPs. The HBEC cells were exposed to 1, 10 and 20 μg/ml (0.3–6.3 μg/cm²) of the different NPs in primary sizes 5 and 50 nm, respectively, for 48 h after which MN induction was analysed by flow cytometry using the *in vitro* microflow kit (Litron Laboratories). Except from a minor increase for the Ag NPs sized 5 nm, no effects were observed. The positive control etoposide (0.2 μg/ml) induced approximately 15% MN.

excluded from the analysis (24). The flow-cytometry version of scoring MN has not yet been widely employed for NPs, but two studies of Ag NPs (20 and 50 nm) have been published and showed clear MN induction in the HepG2 cells whereas the Caco2 cells were not as sensitive (25,26). Furthermore, we previously used both MN scoring using microscopy as well as flow cytometry in a study on genotoxicity of different TiO_2 NPs (22). We found a good correlation between the methods, although the induction was small (below a 2-fold increase) for the three different materials tested (reference materials NM100, NM101 and NM103 obtained from Joint Research Center in Ispra, Italy).

In general, many studies published until now have reported genotoxicity for various Ag NPs and some of these also elucidate possible size-dependent effects. In the present study, we observed genotoxicity (comet assay) for both particle sizes tested (5 and 50 nm). This is in line with our previous study on BEAS-2B cells showing increased DNA damage (comet assay) for all particle sizes of Ag NPs tested (10, 40, 75 nm citrate coated as well as 50–200 nm non-coated) at non-cytotoxic conditions (8). Similarly to the present study, Souza *et al.* compared genotoxicity of Ag NPs in particle sizes of 10 and 100 nm and observed a clear induction in DNA breaks (comet assay) for both sizes, whereas only a slight increased MN induction was observed (13). Huk and colleagues (2014) investigated size-dependent genotoxicity of Ag NPs (50, 80 and 200 nm) using A549 cells and found that the 50 nm-sized particles were the most effective in inducing DNA strand breaks (comet assay), whereas the larger particles were more prone to cause mutations (*hprt* mutations in V79-4 cells) (9). The smaller sized Ag NPs were also most genotoxic in a comprehensive study by Guo and colleagues investigating size- (20, 50 and 100 nm) and coating- (citrate and polyvinylpyrrolidone) dependent genotoxicity of Ag NPs. For MN formation as well as mutations (mouse lymphoma assay), the smallest Ag NPs (20 nm) were most potent although the differences were less pronounced when the dose was expressed as surface area (16). A higher genotoxic potency of smaller Ag NPs (when using mass as a dose metric) has also been shown in other studies (14,15). Taken together, a substantial number of *in vitro* studies show genotoxicity of Ag NPs, but the role of size is not completely clear, probably due to variations in parameters such as agglomeration, cell dose and Ag ion release in the different studies. Genotoxicity in animal studies is less studied and also more controversial (27). A recent review summarised the findings from 16 *in vivo* studies and concluded that genotoxicity was reported in the majority of them (12).

An interesting question relates to whether the genotoxicity is caused by the Ag NPs or the released Ag^+ ions. Previous studies have suggested an importance of a 'Trojan horse effect', i.e. a high uptake of NPs followed by intracellular release of Ag^+ (7,8,28). The Ag NP-exposed cells can thus be affected both by the NPs and the released ions. Two recent studies have shown genotoxicity of Ag NPs as well as Ag ions/complexes (from added $AgNO_3$) (16,29), but different underlying mechanisms were indicated. Likely, small Ag NPs form ROS, such as hydroxyl radicals (29,30), whereas the Ag ions/complexes react with thiol groups leading to e.g. depletion of glutathione.

In contrast to the Ag NPs, we observed clear size-dependent DNA damage (comet assay) for the Au NPs in the sense that only the smallest (5 nm) particles were active, which is perfectly in line with another study comparing genotoxicity of Au NPs of different size (5, 20 and 50 nm) (31). Interestingly, in this study also *in vivo* genotoxicity using the MN assay was performed and the results showed no MN induction following the standard procedure (MN frequencies in bone marrow cells of mice after 4-day intravenous administration), whereas an evident induction was observed after repeated long term exposure (14 repeated doses) (31). MN induction as well as DNA strand breaks have also been reported for Au NPs sized both 5 and 15 nm (17). A recent study showed, however, lack of MN induction of Au NPs but an apparent response using the comet assay (32). The

authors concluded that the response observed in the comet assay may be 'false positive' due to additional DNA damage formed during the assay performance as a result of direct interaction between Au NPs and nucleoid DNA (32). This has also been suggested in other studies (33,34) and such interactions may indeed result in some additional DNA breaks. To what extent such interactions cause false positives, rather than slightly exaggerated damage, remains to be elucidated.

An important question is what mechanism that may underlie genotoxicity of small Au NPs. Clearly, Au NPs are generally considered non-toxic, but results are inconclusive in particular for sizes below 3–5 nm (35). Pan and colleagues demonstrated, e.g. that Au NPs in the size range of 0.8–1.8 nm were highly toxic whereas 15 nm-sized Au NPs were relatively non-toxic (36). For Au NPs with a size of 1.4 nm, a direct interaction with DNA has been suggested to be an important mechanism for the toxicity observed (37). Small Au NPs are also known to be catalytically active (38). The exact mechanism for size-dependent genotoxicity of Au NPs is thus still not totally defined.

In contrast to the Au NPs, the Pt NPs showed a size-dependent effect in the sense that the 50 nm Pt NPs caused a small increase in DNA damage compared to the 5 nm-sized NPs. Pt NPs are not very well studied, but in a previous study on keratinocytes a slight induction of DNA strand breaks were observed for Pt NPs sized 5.8 nm, an effect that was more pronounced compared to observations made for Pt NPs sized 57 nm (19). Furthermore, Asharani *et al.* reported genotoxicity of Pt NPs (size approximately 5–8 nm) using both the comet assay and the MN assay, although observed effects in the comet assay were mainly pronounced for higher doses (40–180 µg/ml) (5). Other studies have reported that Pt NPs are seemingly non-toxic (20,39), thus, the full understanding on Pt NP (geno)toxicity remains to be elucidated.

Taken together, by using the comet assay, our study shows DNA strand breaks from Ag NPs, without any apparent differences due to particle size, whereas effects from Au NPs were clearly size-dependent in the sense that only the 5 nm sized particles were active. For Pt NPs, a small increase in DNA breaks was observed for the 50 nm-sized NPs.

Supplementary data

Supplementary data are available at *Mutagenesis* Online.

Funding

This study was supported by the Swedish Research Council (grant number 2014–4598) and Erasmus+ traineeship for J.L. Additional grants from the Swedish Research Council (grant numbers 2013–5621 and 2015–04177) are also acknowledged.

Acknowledgement

Zheng Wei, at KTH, is highly acknowledged for the electrophoretic mobility measurements and Dr Kjell Hultenby, KI, for TEM imaging.

Conflict of interest statement: None declared.

References

1. McGillicuddy, E., Murray, I., Kavanagh, S., *et al.* (2017) Silver nanoparticles in the environment: Sources, detection and ecotoxicology. *Sci. Total Environ.*, 575, 231–246.
2. Cobley, C. M., Chen, J., Cho, E. C., Wang, L. V. and Xia, Y. (2011) Gold nanostructures: a class of multifunctional materials for biomedical applications. *Chem. Soc. Rev.*, 40, 44–56.
3. Ravindra, K., Bencs, L. and Van Grieken, R. (2004) Platinum group elements in the environment and their health risk. *Sci. Total Environ.*, 318, 1–43.
4. Yamada, M., Foote, M. and Prow, T. W. (2015) Therapeutic gold, silver, and platinum nanoparticles. *Wiley Interdiscip. Rev. Nanomed. Nanobiotechnol.*, 7, 428–445.
5. Asharani, P. V., Xinyi, N., Hande, M. P. and Valiyaveettil, S. (2010) DNA damage and p53-mediated growth arrest in human cells treated with platinum nanoparticles. *Nanomedicine (Lond).*, 5, 51–64.
6. Hackenberg, S., Scherzed, A., Kessler, M., *et al.* (2011) Silver nanoparticles: evaluation of DNA damage, toxicity and functional impairment in human mesenchymal stem cells. *Toxicol. Lett.*, 201, 27–33.
7. Jiang, X., Miclăuş, T., Wang, L., Foldbjerg, R., Sutherland, D. S., Autrup, H., Chen, C. and Beer, C. (2015) Fast intracellular dissolution and persistent cellular uptake of silver nanoparticles in CHO-K1 cells: implication for cytotoxicity. *Nanotoxicology*, 9, 181–189.
8. Gliga, A. R., Skoglund, S., Wallinder, I. O., Fadeel, B. and Karlsson, H. L. (2014) Size-dependent cytotoxicity of silver nanoparticles in human lung cells: the role of cellular uptake, agglomeration and Ag release. *Part. Fibre Toxicol.*, 11, 11.
9. Huk, A., Izak-Nau, E., Reidy, B., Boyles, M., Duschl, A., Lynch, I. and Dušinska, M. (2014) Is the toxic potential of nanosilver dependent on its size? *Part. Fibre Toxicol.*, 11, 65.
10. Che, B., Luo, Q., Zhai, B., Fan, G., Liu, Z., Cheng, K. and Xin, L. (2017) Cytotoxicity and genotoxicity of nanosilver in stable GADD45α promoter-driven luciferase reporter HepG2 and A549 cells. *Environ. Toxicol.*, 32, 2203–2211.
11. Asare, N., Duale, N., Slagsvold, H. H., *et al.* (2016) Genotoxicity and gene expression modulation of silver and titanium dioxide nanoparticles in mice. *Nanotoxicology*, 10, 312–321.
12. Fewtrell, L., Majuru, B. and Hunter, P. R. (2017) A re-assessment of the safety of silver in household water treatment: rapid systematic review of mammalian in vivo genotoxicity studies. *Environ. Health*, 16, 66.
13. Souza, T. A., Franchi, L. P., Rosa, L. R., da Veiga, M. A. and Takahashi, C. S. (2016) Cytotoxicity and genotoxicity of silver nanoparticles of different sizes in CHO-K1 and CHO-XRS5 cell lines. *Mutat. Res. Genet. Toxicol. Environ. Mutagen.*, 795, 70–83.
14. Vecchio, G., Fenech, M., Pompa, P. P. and Voelcker, N. H. (2014) Lab-on-a-chip-based high-throughput screening of the genotoxicity of engineered nanomaterials. *Small*, 10, 2721–2734.
15. Butler, K. S., Peeler, D. J., Casey, B. J., Dair, B. J. and Elespuru, R. K. (2015) Silver nanoparticles: correlating nanoparticle size and cellular uptake with genotoxicity. *Mutagenesis*, 30, 577–591.
16. Guo, X., Li, Y., Yan, J., *et al.* (2016) Size- and coating-dependent cytotoxicity and genotoxicity of silver nanoparticles evaluated using in vitro standard assays. *Nanotoxicology*, 10, 1373–1384.
17. Di Bucchianico, S., Fabbrizi, M. R., Cirillo, S., Uboldi, C., Gilliland, D., Valsami-Jones, E. and Migliore, L. (2014) Aneuploidogenic effects and DNA oxidation induced in vitro by differently sized gold nanoparticles. *Int. J. Nanomedicine*, 9, 2191–2204.
18. Paino, I. M., Marangoni, V. S., de Oliveira, R. d. e. C., Antunes, L. M. and Zucolotto, V. (2012) Cyto and genotoxicity of gold nanoparticles in human hepatocellular carcinoma and peripheral blood mononuclear cells. *Toxicol. Lett.*, 215, 119–125.
19. Konieczny, P., Goralczyk, A. G., Szmyd, R., *et al.* (2013) Effects triggered by platinum nanoparticles on primary keratinocytes. *Int. J. Nanomed.*, 8, 3963–3975.
20. Elder, A., Yang, H., Gwiazda, R., Teng, X., Thurston, S., He, H. and Oberdorster, G. (2007) Testing nanomaterials of unknown toxicity: an example based on platinum nanoparticles of different shapes. *Adv. Mater.*, 19, 3124–3129.
21. Skoglund, S., Hedberg, J., Yunda, E., Godymchuk, A., Blomberg, E. and Odnevall Wallinder, I. (2017) Difficulties and flaws in performing accur-

ate determinations of zeta potentials of metal nanoparticles in complex solutions-Four case studies. *PLoS One*, 12, e0181735.

22. Di Bucchianico, S., Cappellini, F., Le Bihanic, F., Zhang, Y., Dreij, K. and Karlsson, H. L. (2017) Genotoxicity of TiO2 nanoparticles assessed by mini-gel comet assay and micronucleus scoring with flow cytometry. *Mutagenesis*, 32, 127–137.
23. Wichmann, H., Anquandah, G. A., Schmidt, C., Zachmann, D. and Bahadir, M. A. (2007) Increase of platinum group element concentrations in soils and airborne dust in an urban area in Germany. *Sci. Total Environ.*, 388, 121–127.
24. Avlasevich, S., Bryce, S., De Boeck, M., Elhajouji, A., Van Goethem, F., Lynch, A., Nicolette, J., Shi, J. and Dertinger, S. (2011) Flow cytometric analysis of micronuclei in mammalian cell cultures: past, present and future. *Mutagenesis*, 26, 147–152.
25. Sahu, S. C., Njoroge, J., Bryce, S. M., Yourick, J. J. and Sprando, R. L. (2014) Comparative genotoxicity of nanosilver in human liver HepG2 and colon Caco2 cells evaluated by a flow cytometric in vitro micronucleus assay. *J. Appl. Toxicol.*, 34, 1226–1234.
26. Sahu, S. C., Njoroge, J., Bryce, S. M., Zheng, J. and Ihrie, J. (2016) Flow cytometric evaluation of the contribution of ionic silver to genotoxic potential of nanosilver in human liver HepG2 and colon Caco2 cells. *J. Appl. Toxicol.*, 36, 521–531.
27. SCENIHR (2014) *Opinion on Nanosilver: Safety, Health and Environmental Effects and Role in Antimicrobial Resistance*. https://ec.europa.eu/health/scientific_committees/emerging/docs/scenihr_o_039.pdf.
28. Cronholm, P., Karlsson, H. L., Hedberg, J., Lowe, T. A., Winnberg, L., Elihn, K., Wallinder, I. O. and Möller, L. (2013) Intracellular uptake and toxicity of Ag and CuO nanoparticles: a comparison between nanoparticles and their corresponding metal ions. *Small*, 9, 970–982.
29. Li, Y., Qin, T., Ingle, T., Yan, J., He, W., Yin, J. J. and Chen, T. (2017) Differential genotoxicity mechanisms of silver nanoparticles and silver ions. *Arch. Toxicol.*, 91, 509–519.
30. Carlson, C., Hussain, S. M., Schrand, A. M., Braydich-Stolle, L. K., Hess, K. L., Jones, R. L. and Schlager, J. J. (2008) Unique cellular interaction of silver nanoparticles: size-dependent generation of reactive oxygen species. *J. Phys. Chem. B*, 112, 13608–13619.
31. Xia, Q., Li, H., Liu, Y., Zhang, S., Feng, Q. and Xiao, K. (2017) The effect of particle size on the genotoxicity of gold nanoparticles. *J. Biomed. Mater. Res. A*, 105, 710–719.
32. George, J. M., Magogotya, M., Vetten, M. A., Buys, A. V. and Gulumian, M. (2017) From the cover: an investigation of the genotoxicity and interference of gold nanoparticles in commonly used in vitro mutagenicity and genotoxicity Assays. *Toxicol. Sci.*, 156, 149–166.
33. Ferraro, D., Anselmi-Tamburini, U., Tredici, I. G., Ricci, V. and Sommi, P. (2016) Overestimation of nanoparticles-induced DNA damage determined by the comet assay. *Nanotoxicology*, 10, 861–870.
34. Karlsson, H. L., Di Bucchianico, S., Collins, A. R. and Dusinska, M. (2015) Can the comet assay be used reliably to detect nanoparticle-induced genotoxicity? *Environ. Mol. Mutagen.*, 56, 82–96.
35. Dykman, L. and Khlebtsov, N. (2012) Gold nanoparticles in biomedical applications: recent advances and perspectives. *Chem. Soc. Rev.*, 41, 2256–2282.
36. Pan, Y., Neuss, S., Leifert, A., Fischler, M., Wen, F., Simon, U., Schmid, G., Brandau, W. and Jahnen-Dechent, W. (2007) Size-dependent cytotoxicity of gold nanoparticles. *Small*, 3, 1941–1949.
37. Tsoli, M., Kuhn, H., Brandau, W., Esche, H. and Schmid, G. (2005) Cellular uptake and toxicity of Au55 clusters. *Small*, 1, 841–844.
38. Daniel, M. C. and Astruc, D. (2004) Gold nanoparticles: assembly, supramolecular chemistry, quantum-size-related properties, and applications toward biology, catalysis, and nanotechnology. *Chem. Rev.*, 104, 293–346.
39. Horie, M., Kato, H., Endoh, S., *et al*. (2011) Evaluation of cellular influences of platinum nanoparticles by stable medium dispersion. *Metallomics*, 3, 1244–1252.